Research Square

Preprints are preliminary reports that have not undergone peer review.
They should not be considered conclusive, used to inform clinical practice,
or referenced by the media as validated information.

Reactive transport modelling of element leach behavior in high-level radioactive waste disposal glass

Ping Chen
china institute of atomic energy
Shengchao Li
china institute of atomic energy
Mingfang Zhou
china institute of atomic energy
Dongshen Xu
china institute of atomic energy
Chengming Shang
china institute of atomic energy
Duo Zhou
china institute of atomic energy
Guoxin Tian
china institute of atomic energy
Shengheng Tan
china institute of atomic energy
Yu Zhang
zhangyu1@cnncmail.cn

china institute of atomic energy

Article

Keywords: borosilicate glass, leach mechanism, reactive leach model, chemical reaction, diffusion

Posted Date: May 14th, 2026

DOI: https://doi.org/10.21203/rs.3.rs-9571045/v1

License: This work is licensed under a Creative Commons Attribution 4.0 International License.
Read Full License

Additional Declarations: No competing interests reported.

Abstract

Deep geological disposal based on multi-barriers system is internationally accepted as final disposal technique for high-level radioactive waste. Solidification of high-level radioactive waste after reprocess is the first barrier for repositories in some countries, such as China and France. Vitrification, as one of the solidification technology, has been widely investigated. Leaching behavior modeling is of utmost importance for long-term safety assessment of a repository. Leaching experiment is performed in deionized water and further a reactive leach modeling of borosilicate glass is studied in this paper. Based on leaching experimental data in aqueous solution and glass surface, borosilicate glass leach model is coupled chemical reactions with nuclide diffusion process. Leached silicon (Si), boron (B) and uranium (U) are satisfactorily simulated with suitable parameter sets, which are glass porosity, glass dissolution reaction, reaction constant and rate, effective diffusion coefficient of silicon, boron and uranium. Reactive leach modeling unveils that the leach mechanism of borosilicate glass undergoes three stages. Glass dissolution at interface leads to rapid B, Si and U increasing in solution at first stage. Followed with water solution diffusing into glass pore, glass dissolves in pore and dissolved B, Si and U diffuses out into solution, resulting in a much slower increasing. At final stage, B, Si and U in solution reach a plateau stage due to glass dissolution equilibrium achieved. Uranium, as one of the main radioactive component in high-level radioactive waste, its leach mechanism is so far firstly reported. This model provides basic quantitative method and data for long-term safety assessment of the vitrified solid and further the repository. Further development of reactive leach model is needed in order to couple cation exchange and surface reaction to explain leaching behavior of cations and radionuclides in borosilicate glass and the formation of gel layer.

Introduction

Deep geological disposal based on multi-barriers system is internationally accepted as final disposal technique for high-level radioactive waste. Significant progress has been achieved internationally and Finland is in a leading position. First repository has been built up and the trial run of final disposal is undergoing[1], in which the joint functionality of all the equipment, systems, processes, and organizations were tested without real spent nuclear fuel. In this repository spent fuel is supposed to be directly encapsulated in canister without reprocess. In China and France, in order to recover useful nuclides, reprocess of high-level radioactive waste (HLW) following solidification strategy is selected for the disposal of HLW[2–7]. Glass solidification has been proved to be a suitable method to immobilizing all elements present in solution after reprocess[8–25]. The HLW is currently immobilized using Na–Al–P glass in Russia[26–28] and Na–B–Si glass elsewhere[29]. Vitrification of HLW with borosilicate glass is confirmed as technical approach to HLW repository in China. Glass in repository is supposed to expose to groundwater after HLW canister failure, during which glass may corrode under complex processes, finally leading to leach of radionuclides packaged in glass and transport in groundwater. A comprehensive understanding of borosilicate glass corrosion behavior in water is essential to predict and evaluate the long-term behavior of radionuclides in near field of repository. Extensive investigations

have been conducted for borosilicate glass corrosion behavior[30–37]. Complex processes may control its corrosion, during which generally start with a fast corrosion rate, follow with a drop corrosion rate resulting from gel formation, finally reach a plateau with very slow corrosion rate. Glass composition is the utmost important factor in affecting glass chemical durability[38–40]. Radiation[41, 42] and temperature[43, 44] were confirmed to influence the structure of borosilicate glass and further influence its corrosion behavior. In recent years, the effect of doping Mg[45], Al[46, 47], Ag[48], Ca[49] on glass structure and chemical durability has also been investigated. A slower matrix dissolution and formation of gel is confirmed by doping Al[47]. Ca probably form a more passivating gel layer, leading to less glass altered in solution[49]. Gel layer formation has been recognized as the main reason for a slower residual corrosion rate[50]. A Monte Carlo method has been developed to elucidate the leach mechanism of borosilicate[51–53]. It provides atomic-level insight to corrosion behavior of borosilicate. Further effort has been made to couple reaction and diffusion processes in Monte Carlo simulation[54]. Molecular dynamics simulation is another powerful tool to reveal the mechanism between glass and water interface[45, 55, 56]. It shows Na is directly dissolved and B(III) is more prone to non-dissociative adsorption of water than B(IV), followed by dissociative adsorption and ultimately forms terminal B – OH and silanol H – NBO bond[56]. While Ca cannot leave glass surface[55].

Through Monte Carlo and Molecular dynamics simulations, a qualitative descript of borosilicate glass corrosion mechanism is achieved. That is B and Na can dissolve into solution, but Si and other ion are not as soluble as B. They may reorganize or precipitate at glass surface forming the gel layer, which in turn blocks the transport of soluble species, resulting in a slower residual corrosion rate. However, these simulations are based atomic reactions, important processes such as diffusion of soluble species is not taken into account. Although it is claimed that diffusion and reactions are coupled in the Monte Carlo simulation[51], diffusion is considered in a way based on final Si distribution in the altered layer rather than transport of species. In this study, leach experiment of borosilicate glass is performed in deionized water at room temperature. Furthermore, a novel reactive leach model is developed, in which diffusion of dissolved species are coupled with glass dissolution reaction. Borosilicate glass is assumed to be homogeneous and porous medium. Parameters that control the leach of element are extensively discussed, for example, the equilibrium constant and the reaction rate of dissolution reaction, the diffusion coefficient of dissolved species. Optimization of parameters is achieved by manually adjusting these parameters mentioned above. Leach mechanism of uranium was firstly reported in literature.

Results

Reactive leach model compared with experiment data

A reference reactive model is consist of composition of glass, glass dissolution reaction, dissolution reaction rate, effective diffusion coefficient of B, Si and U, and geometry, which based on experiment setup and always keep constant. In the simplest model, only parameters discussed above are left to

adjust and the other parameters are kept unchanged. By manually adjusting these parameters, best fit is achieved for experimental data in deionized water solution as shown in Fig. 1. Its corresponding optimized parameters is list in Table 1. Model output in Fig. 1a and 1b is in good agreement with experimental data, including Si, B and U concentration in leach solution. This indicates that this reactive leach model is successful in describing leach behavior of Si, B and U in deionized water, even though little discrepancy with experimental data still exist for Si, B and U concentration at the initial quick increasing stage, especially for U. This bigger discrepancy for U may result from the bigger uncertainty as shown in Fig. 1b after 140 days. Other mechanism that may lead to this could not be ruled out.

Table 1
Best fit parameters for reactive leach model

reaction	**SiO_2*0.93 B_2O_3*0.01UO_3 + 3.78 H_2O == 1.86 $B(OH)_3$ + $HSiO_3^-$ + 0.98 H^+ + 0.01 UO_2^{2+}**
parameters	
reaction rate R (mol/m^2/s)	0.05
equilibrium constant log K	Log K =-10.3
effective diffusion coefficient of Si (m^2/s)	2.6×10^{-13}
effective diffusion coefficient of B (m^2/s)	1.0×10^{-13}
effective diffusion coefficient of U (m^2/s)	5.0×10^{-13}

In other hand, morphological difference has been observed only at a depth of a few micrometers from interface between glass and solution by SEM (Fig. 2a). With further characterization by SEM-EDX, a decline trend of Si is obvious in the surface (Fig. 1b). The reactive leach model gives the similar decline trend of glass volume fraction in the several micrometers depth from surface, which is shown in Fig. 1c. This further suggests the success of this model in explaining the experimental observation.

Influence of equilibrium constant

Figure 3 shows the influence of three equilibrium constants of glass dissolution reaction, where value of reaction rate, effective diffusion coefficient of B, Si and U are kept unchanged as 0.05 mol/m^2/s, 1.00×10^{-13} m^2/s 2.60×10^{-13} m^2/s and 5.00×10^{-13} m^2/s, respectively. As shown in Fig. 3a, 3b and 3c, similar trend is obviously observed for Si, B and U, that the concentration in the solution undergoes three stage. Firstly, the concentration in solution increases rapidly. This may result from the large interface between solution and glass. Secondly, the concentration increasing becomes quite slowly, which may result from dissolved Si, B and U in glass pore diffusing out into solution slowly. Finally, the

concentration reaches a plateau and no more increase is observed after that during the simulation time. In Fig. 3a, 3b and 3c, it is obvious that a bigger equilibrium constant of glass dissolution reaction results in a higher leached concentration for Si, B and U. This means the final Si, B and U concentration in solution is controlled by the equilibrium constant of glass dissolution reaction. Whereas in other hand, longer time seems need for reaching its equilibrium in case with bigger equilibrium constant. This suggests that dissolution reaction is kineticly controlled.

Influence of reaction rate

The influence of reaction rate on Si, B, and U concentration is shown in Fig. 4a, 4b and 4c, with equilibrium constant, effective diffusion coefficient of B, Si and U keeping the same as -10.3, 1.00×10^{-13} m^2/s 2.60×10^{-13} m^2/s and 5.00×10^{-13} m^2/s, respectively. Apparently, three stage are still observed for the three reaction rates, and the concentration in plateau stage is same for both Si and B. A smaller concentration of U in smaller reaction rate in not quite understood (Fig. 4c). It may result from the low fraction composition of U in glass compared to B and Si. In this case, smaller dissolution rate leads dissolved U in deeper glass not saturated. Dissolved U at the reaction frontier can diffuse toward both deeper glass and leach solution, leading to low concentration in solution with smaller reaction rate as shown in Fig. 4c. Regards to Si and B, impact of vary dissolution reaction rate on leach solution is significant for the time needed for leached concentration reaching plateau. This indicates that a rapid increase concentration at initial stage is mostly controlled by the reaction rate. As shown in Fig. 4a, 4b and 4c, reaction rate increasing from 0.05 to 0.5 $mol/m^2/s$ makes no difference to the concentration of Si, B, and U. This suggests that reaction rate with value of 0.05 $mol/m^2/s$ is fast enough. It is no more the dominant mechanism controlling the dissolution of glass. Other processes such as diffusion may become the dominant process controlling leach behavior of Si, B, and U than dissolution reaction when reaction rate lager than 0.05 $mol/m^2/s$.

Influence of effective diffusion coefficient of Si, B and U

For the influence study of effective diffusion coefficient of Si and B, three cases are taken into consideration, in which equilibrium constant and reaction rate have value of -10.3 and 0.05 $mol/m^2/s$. three cases are the influence of D_e of Si alone (Fig. 5a, 5b, 5c, D_e of B with value of 1.00×10^{-13} m^2/s), of B alone (Fig. 5d, 5e, 5f, D_e of Si with value of 2.60×10^{-13} m2/s), and that of both Si and B (Fig. 5g, 5h, 5i) on Si, B and U concentration in leach solution. Almost no Influence of D_e of U on Si, B and U concentration is observed (shown in supplementary information in Fig S1), which may indicate U in this reactive leach model was controlled by other factors, for instance the dissolution reaction or glass composition. Diffusion process alone in glass pore is not significant for U. As shown in Fig. 5a, 5b, 5c, and 5d, 5e, 5f, changes of either D_e of Si or B, similar influence on Si and B is observed, which is more time needed for leached concentration to reach plateau with decreasing effective diffusion coefficient but equilibrium concentration keeping unchanged. Discrepancy is observed for impact on U

concentration, in which decreasing effective diffusion coefficient leads to higher leached U concentration although more time needed to reach equilibrium. This may result from the different amount of Si, B and U in glass composition. As mentioned above, compared to Si and B, U in glass is much small, resulting in U concentration not saturated however Si and B quickly being saturated. This means even although increasing D_e of either Si or B provides more dissolved U, some dissolved U is diffused into glass pore in deeper place, leading to less U in solution (which is what observed in Fig. 5c and 5f). Compared Fig. 5g, 5h and 5i with 5a, 5b, 5c and 5d, 5e, 5f, significant influence is observed for variation of D_e for both Si and B at same time on Si, B and U concentration. Decreasing D_e of both Si and B leads to much slowly increasing of Si and B concentration. Same influence is observed for U concentration with various D_e of either Si or B, That is smaller leached U concentration with increased D_e. It is worth noted that the influence of D_e of Si and B looks similar with reaction rate, where a bigger D_e or R gives a fast increasing concentration at the beginning. This may bring difficulty to simulation for parameters optimization according to experimental data.

Discussion

In leach solution as shown in Fig. 1, concentration of Si, B and U finally reach a plateau, which suggests that an equilibrium assumption of Si, B and U is reasonable. Although a slower residual rate is extensively discussed[57] and attributed to the formation of gel layer. In this reactive leach model, gel layer is not yet being considered. A homogeneous composition was obtained based on the final leached concentration of Si, B and U, which gives a composition of SiO_2*0.93 B_2O_3*0.01UO_3. The dissolution reaction rate, which is considered as gradually decreased to a very small value[47], is keep constant in this model. Assuming all parameters assumptions in Table 1 are reasonable, the reactive leach model with parameters in Table 1 is good enough to predict Si, B and U leach behavior in deionized water. More information about the leach process is available from the model. As shown in Fig. 6a, H_2O quickly diffuse into borosilicate glass and reach equilibrium within 1 day. H_2O react with glass at both the interface and glass pore, leading B and Si dissolved and leached out into solution (as shown in Fig. 6b and 6c). As indicated in Fig. 6b, B and Si show a similar trend in both solution and glass pore. This is reasonable since B and Si have similar function and similar amount in glass, and the D_e is in the same order of magnitude. Figure 6d suggests a bigger difference for U behavior. As discussed above, compared with Si and B, U is not saturated in both glass pore and solution, U would diffuse into pore in deeper place and in solution. This model indicates that glass is first dissolved at the interface since a lager contact surface leading to a rapid increasing concentration of Si, B and U in solution. Then water diffuses into pore and further dissolves more glass in pore. Because dissolution equilibrium is easy to reach in glass pore since porosity is very small, result in slowing increasing in solution, indicating diffusion process being dominate. Finally only several micrometer of glass was obviously dissolved (as shown in Fig. 6e), which is agreement with observation from SEM-EDX result (as shown in Fig. 2b).

In summary, for the first try, a reactive leach model is proposed to unveil the leach behavior of B, Si and U, in which glass dissolution reaction and diffusion process are coupled together. Modeling result is in

perfect agreement with experimental result, and provides with more information inside glass. B and Si is firstly quickly dissolved at the interface, result in a rapid increased B and Si concentration in solution. Following dissolution and diffusion in glass pore lead to a slowly increased after the initial stage. Finally, B and Si concentration is controlled by dissolution equilibrium, where a steady stage is reached with maximum B and Si concentration. Leach behavior of U is firstly studied and reported. Since small amount of U incorporated in glass, dissolved U in glass pore is not saturated and can diffuse toward deeper pore and solution, resulting in different behavior respond to various D_e of Si and B. With this model, the long-term behavior B, Si and U in water is possible to predict.

Currently, the reactive leach model is not sophisticated enough. Only leach behavior of B, Si and U is predictable. Further development of this model is necessary for more complicated environment and for other nuclides such as Na, Mg, Ca and so on, whose behavior is similar to sorption behavior of nuclides on mineral surface. One of the consideration is coupling the cation exchange reaction and surface complexation reaction inside the model, which is successful to describe nuclide sorption behavior on mineral surface. Furthermore, precipitate of secondary mineral or reorganized of Si, and B forming the altered/gel layer should be taken into account, which is observed in SEM characterization but bot simulated in this model. With the help of this model, leach behavior of radionuclides in near field in a repository is accessible for in-situ condition over long time.

Methods

Borosilicate glass preparation

The borosilicate glass containing simulated high level waste is prepared by melting-annealing method. The basic glass frits and waste simulants (at a waste loading of 22 wt% on an oxide basis) are mechanically mixed and homogenized for 20 min in an agate mortar. The mixture is then transferred into corundum crucibles and heated in a preheated electric furnace at 1150°C for 3 h. Subsequently, the glass melts are poured onto a preheated graphite mold and annealed for 1 h at 500°C, and cooled to room temperature at 1°C min^{-1}. The prepared glass bars are further sliced to thin slices of 1 mm thickness and polished to 1200 mesh with SiC grits. Glass composition is shown in Table S1 in supplementary information[58].

Leach experiment

The sliced and polished borosilicate glass is cubic with parameters of 1.5cm×0.6cm×0.6cm. It is soaked in 25 ml vessel at 25 ℃ during leach experiment. 20 ml of deionized water is used as soaking solution. Samples are taken from soaking solution at a series of time point and elements concentration are measured by Inductively Coupled Plasma Mass Spectrometry (ICP-MS). Immersed borosilicate glasses are dried at 110 ℃ for 24 hours before solid characterization. Scanning electron microscopy (SEM) and energy-dispersive X-ray spectroscopy (EDX) are applied for glass morphology characterization and

elements composition measurement at the surface. X-ray diffraction (XRD) is applied to confirm phase transformation and results were shown in Fig S2 in supplementary information.

Reactive leach model

Mathematical theory

Leach behavior of elements from borosilicate glass is modeled by coupling species diffusion and chemical reactions in PFLOTRAN platform, which is one of the advanced reactive transport code[59]. The governing equations are elaborated in detail in a previous work[60] and more detail in PFLOTRAN website. In the leach experiment, there is no advection. The governing mass conservation equations for solute mass in liquid phase is simplified as Eqs. 1 and 2.

$$\frac{\partial}{\partial t}\left(\varphi \sum \psi_j\right) - \nabla \bullet \sum (\varphi D \bullet \nabla \psi_j) = -\frac{\partial \mathrm{S_j}}{\partial t} - \sum {}_m\nu_{jm} I_m$$

1

$$\frac{\partial \varphi_m}{\partial t} = V_m I_m$$

2

for minerals with molar volume V_m, reaction rate I_m and volume fraction φ_m. The term involving S_j describes sorption processes. The quantity ψ_j denotes the total concentration of the j^{th} primary species A_j^{pri}. φ is the porosity. D is the diffusion coefficient.

Chemical reaction

These involved chemical reactions consist of two type. One type is reaction between the solid glass and the surrounding solution. It may include glass dissolution, re-precipitate, ion exchange and surface reaction. The other is reactions between liquid species. In order to simplify the model and ensure its good performance, only the experiment result of deionized water was used in this model. Furthermore, the borosilicate glass is assumed to be a uniform porous media. As a first trial, only the primary element B and Si of glass and U (represent of active waste), are taken into account. The composition of borosilicate glass is supposed to be SiO_2*0.93 B_2O_3*0.01UO_3, which calculated based on final leached element concentration. The primary species for B and Si in the simulation are set to be $B(OH)_3$ and $HSiO_3^-$. And that for U is UO_2^{2+}. Therefore, the dissolution reaction of glass is shown as Eq. 3. The concentration of B, Si and U are obtained by ICP-MS. That means no species information is available. So no further reaction for $B(OH)_3$, $HSiO_3^-$ and UO_2^{2+} are considered in aqueous form in the model.

SiO_2*0.93 B_2O_3*0.01UO_3 + 3.78 H_2O = = 1.86 $B(OH)_3$ + $HSiO_3^-$ + 0.98 H^+ + 0.01 UO_2^{2+} (3)

Diffusion

The leach experiment is performed in a vessel with a 1.5cm×0.6cm×0.6cm glass soaking in 20 ml water (as shown in Fig. 7a), which is equivalent to the simplified geometry with 1cm×2cm interface (as shown in Fig. 7b), the length of solution is recalculated from the section of interface and the solution volume, which is 100 mm. Furthermore, the simplified geometry is discretized as following: The glass was discretized into 1000×1um, the solution was divided into two parts for the convergence of simulation. That is 100 small pieces with 0.01 mm for each closed to interface of glass and solution, following 100 bigger pieces with 0.99 mm for each.

Advection is not possible in the leach experiment. Diffusion occurs for every species in the aqueous form in the glass pore and in the solution. That is $B(OH)_3$, $HSiO_3^-$, UO_2^{2+}, H^+ and H_2O in this model. Since porosity of glass was not measured and not reported in literature, a relative small value is assigned and that in liquid solution is assumed to be 1, meaning all space is available for diffusion in aqueous solution. Tortuosity factor, which is countdown of tortuosity, in glass and liquid solution is set to 1 and 1000000, respectively. A big tortuosity factor in liquid is to ensure species mixed homogeneously and instantaneously. The effective diffusion coefficient is the product of molecular diffusion, porosity and tortuosity factor.

Parameters

A reference model is provided first to elucidate how the reactive leach model works. A reference model includes several parts, which is the geometry, materials properties, chemical reactions and diffusion. Parameters for each part are list in Table 2. In the initial condition of the reference model, SiO_2*0.93 B_2O_3*0.01UO_3 only exists in glass with a volume fraction of 0.9995, and deionized water is only exist in solution. Correspondingly, the porosity in glass and in solution is 0.0005 and 1, respectively. Therefore, leach experiment goes through following processes. Firstly, water interacts with glass at the interface causing glass dissolution with reaction rate R. At meantime, dissolved $B(OH)_3$, $HSiO_3^-$, and UO_2^{2+} diffuses into the solution quickly, which lead quickly increasing concentration of B, Si and U in solution. Secondly, water diffuses into glass along with pore with D_0 (H_2O), causing more glass dissolved and diffused out into solution. Finally, since the solution volume is limited as 20 mL, dissolution reaction reaches equilibrium, leading to a constant concentration of B, Si and U.

Table 2
Parameters for reactive leach model

	Glass	Solution
	Geometry	
Cross section (cm^2)	2	2
Length (mm)	1	100
Grid (mm)	1000*0.001	100*0.01 + 100*0.99
	Materials properties	
Component	SiO_2*0.93 B_2O_3*0.01UO_3	H_2O
porosity	0.0005	1
Tortuosity factor	1	1000000
	Chemical reaction	
Glass dissolution	SiO_2*0.93 B_2O_3*0.01UO_3 + 3.78 H_2O == 1.86 $B(OH)_3$ + $HSiO_3^-$ + 0.98 H^+ + 0.01 UO_2^{2+}	Log K
Reaction rate ($mol/m^2/s$)	R	
	Diffusion	
$B(OH)_3$ ($10^{-9} m^2/s$)	D_0 ($B(OH)_3$) = D_0^B	
$HSiO_3^-$ ($10^{-9} m^2/s$)	D_0 (H_2SiO_3) = D_0^{Si}	
UO_2^{2+} ($10^{-9} m^2/s$)	D_0 (UO_2^{2+}) = D_0^U	
H^+ ($10^{-9} m^2/s$)	9.31	
H_2O ($10^{-9} m^2/s$)	2.10	

Declarations

Data availability

Data is provided within the manuscript or supplementary information files. Raw data can be provided upon reasonable request.

COMPETING INTERESTS

The authors declare no competing interests.

Author Contribution

Yu Zhang and Shengheng Tan design the leach experiment and supervised the study; Shengchao Li, Mingfang Zhou, and Dongsheng Xu perform the leach experiment and experimental data analysis. Ping Chen conduct the simulation and wrote the manuscript. Chengming Shang, Duo Zhou and Guoxin Tian revise the manuscript. All the authors participated to the scientific discussion and contributed to the editing of the manuscript under its present form.

Acknowledgements

This research is financially supported by the Supportive Funding for Fundamental Research (Grant No. BJ030261223290). The leach experiments, measurements and characterization were carried out in Department of Radiochemistry, China Institute of Atomic Energy. Sincere gratitude to all my colleagues and technicians, who helped us in doing experiments and modelling.

References

1. Sillanpää, T.; Karjanlahti, T., Trial Run ensures safety of final disposal. 2024.
2. Ojovan, M. I., Vitrification as a key solution for immobilisation within nuclear waste management. *Arabian Journal for Science and Engineering* 2025, *50*, (5), 3253–3261.
3. Neeft, E.; Deissmann, G.; Jacques, D., EURAD State-of-the-Art Report: ACED assessment of the chemical evolution at the disposal cell scale—part I—processes at interfaces and evolution at disposal cell scale. *Frontiers in Nuclear Engineering* 2025, *3*, 1433247.
4. Council, N. R.; Earth, D. o.; Geosciences, C. o.; Wastes, S. C. o. V. o. R., *Glass as a Waste Form and Vitrification Technology: Summary of an International Workshop*. National Academies Press: 1997.
5. Lee, C. W.; Shin, S. G.; Kye, Y. U.; Heo, J., Evaluation of thermal stability in deep geological repository and nuclear criticality safety of spent nuclear fuel vitrified in iron phosphate glass. *Annals of Nuclear Energy* 2020, *136*, 107055.
6. Lee, C. W.; Shin, S. G.; Kye, Y. U.; Heo, J. In *Vitrification of the spent nuclear fuel using iron phosphate glasses*, Proceedings of the Conference and Symposium Korean Radioactive Waste Society Autumn Meeting 2018, 2018; 2018; pp 197–198.
7. Mallants, D.; Marivoet, J.; Sillen, X., Performance assessment of the disposal of vitrified high-level waste in a clay layer. *Journal of Nuclear Materials* 2001, *298*, (1–2), 125–135.

8. Vernaz, É.; Bruezière, J., History of nuclear waste glass in France. *Procedia Materials Science* 2014, *7*, 3–9.
9. Gin, S.; Abdelouas, A.; Criscenti, L. J.; Ebert, W. L.; Ferrand, K.; Geisler, T.; Harrison, M. T.; Inagaki, Y.; Mitsui, S.; Mueller, K. T., An international initiative on long-term behavior of high-level nuclear waste glass. *Materials Today* 2013, *16*, (6), 243–248.
10. Caurant, D.; Majérus, O., Glasses and glass-ceramics for nuclear waste immobilization. *Encyclopedia of materials: technical ceramics and glasses* 2021, *2*, 762–789.
11. Charpentier, T.; Martel, L.; Mir, A. H.; Somers, J.; Jégou, C.; Peuget, S., Self-healing capacity of nuclear glass observed by NMR spectroscopy. *Scientific Reports* 2016, *6*, (1), 25499.
12. Peuget, S.; Delaye, J.-M.; Jégou, C., Specific outcomes of the research on the radiation stability of the French nuclear glass towards alpha decay accumulation. *Journal of Nuclear Materials* 2014, *444*, (1–3), 76–91.
13. Gin, S.; Ryan, J. V.; Schreiber, D. K.; Neeway, J.; Cabié, M., Contribution of atom-probe tomography to a better understanding of glass alteration mechanisms: Application to a nuclear glass specimen altered 25 years in a granitic environment. *Chemical Geology* 2013, *349*, 99–109.
14. Guittonneau, C.; Gin, S.; Godon, N.; Mestre, J.; Dugne, O.; Allegri, P., A 25-year laboratory experiment on French SON68 nuclear glass leached in a granitic environment–First investigations. *Journal of Nuclear Materials* 2011, *408*, (1), 73–89.
15. Gin, S.; Guittonneau, C.; Godon, N.; Neff, D.; Rebiscoul, D.; Cabie, M.; Mostefaoui, S., Nuclear glass durability: new insight into alteration layer properties. *The Journal of Physical Chemistry C* 2011, *115*, (38), 18696–18706.
16. Pèlegrin, E.; Calas, G.; Ildefonse, P.; Jollivet, P.; Galoisy, L., Structural evolution of glass surface during alteration: Application to nuclear waste glasses. *Journal of Non-Crystalline Solids* 2010, *356*, (44–49), 2497–2508.
17. Peuget, S.; Broudic, V.; Jégou, C.; Frugier, P.; Roudil, D.; Deschanels, X.; Rabiller, H.; Noel, P., Effect of alpha radiation on the leaching behaviour of nuclear glass. *Journal of nuclear materials* 2007, *362*, (2–3), 474–479.
18. Caurant, D.; Loiseau, P.; Majerus, O.; Aubin-Chevaldonnet, V.; Bardez, I.; Quintas, A., *Glasses, glass-ceramics and ceramics for immobilization of highly radioactive nuclear wastes*. Nova Science Hauppauge: 2007.
19. Rebiscoul, D.; Frugier, P.; Gin, S.; Ayral, A., Protective properties and dissolution ability of the gel formed during nuclear glass alteration. *Journal of Nuclear Materials* 2005, *342*, (1–3), 26–34.
20. Rebiscoul, D.; Van der Lee, A.; Rieutord, F.; Né, F.; Spalla, O.; El-Mansouri, A.; Frugier, P.; Ayral, A.; Gin, S., Morphological evolution of alteration layers formed during nuclear glass alteration: new evidence of a gel as a diffusive barrier. *Journal of Nuclear Materials* 2004, *326*, (1), 9–18.
21. Gin, S.; Ribet, I.; Couillard, M., Role and properties of the gel formed during nuclear glass alteration: importance of gel formation conditions. *Journal of Nuclear Materials* 2001, *298*, (1–2), 1–10.

22. Gin, S.; Mestre, J., SON 68 nuclear glass alteration kinetics between pH 7 and pH 11.5. *Journal of Nuclear Materials* 2001, *295*, (1), 83–96.
23. Techer, I.; Advocat, T.; Lancelot, J.; Liotard, J.-M., Basaltic glass: alteration mechanisms and analogy with nuclear waste glasses. *Journal of Nuclear Materials* 2000, *282*, (1), 40–46.
24. Plodinec, M., Borosilicate glasses for nuclear waste imobilisation. *Glass Technology* 2000, *41*, (6), 186–192.
25. Vernaz, E.; Dussossoy, J., Current state of knowledge of nuclear waste glass corrosion mechanisms: the case of R7T7 glass. *Applied Geochemistry* 1992, *7*, 13–22.
26. Luzhetsky, A. V.; Petrov, V. A.; Yudintsev, S. V.; Malkovsky, V. I.; Ojovan, M. I.; Nickolsky, M. S.; Shiryaev, A. A.; Danilov, S. S.; Ostashkina, E. E., Effect of gamma irradiation on structural features and dissolution of nuclear waste Na–Al–P glasses in water. *Sustainability* 2020, *12*, (10), 4137.
27. Remizov, M.; Kozlov, P.; Borisenko, V.; Dementeva, I.; Blokhin, P.; Samoylov, A., Development of an Algorithm for Estimating the Radionuclide Composition of Vitrified HLW of FSUE “PA “Mayak” for the Purpose of Their Safe Disposal. *Radioact. Waste* 2018, *3*, 87–94.
28. Poluektov, P. P.; Schmidt, O. V.; Kascheev, V. A.; Ojovan, M. I., Modelling aqueous corrosion of nuclear waste phosphate glass. *Journal of Nuclear Materials* 2017, *484*, 357–366.
29. Gin, S.; Jollivet, P.; Tribet, M.; Peuget, S.; Schuller, S., Radionuclides containment in nuclear glasses: an overview. *Radiochimica Acta* 2017, *105*, (11), 927–959.
30. Frankel, G. S.; Vienna, J. D.; Lian, J.; Scully, J. R.; Gin, S.; Ryan, J. V.; Wang, J.; Kim, S. H.; Windl, W.; Du, J., A comparative review of the aqueous corrosion of glasses, crystalline ceramics, and metals. *npj Materials Degradation* 2018, *2*, (1), 15.
31. Gin, S.; Collin, M.; Jollivet, P.; Fournier, M.; Minet, Y.; Dupuy, L.; Mahadevan, T.; Kerisit, S.; Du, J., Dynamics of self-reorganization explains passivation of silicate glasses. *Nature communications* 2018, *9*, (1), 2169.
32. Gin, S.; Jollivet, P.; Fournier, M.; Berthon, C.; Wang, Z.; Mitroshkov, A.; Zhu, Z.; Ryan, J. V., The fate of silicon during glass corrosion under alkaline conditions: a mechanistic and kinetic study with the International Simple Glass. *Geochimica et Cosmochimica Acta* 2015, *151*, 68–85.
33. Gin, S.; Jollivet, P.; Fournier, M.; Angeli, F.; Frugier, P.; Charpentier, T., Origin and consequences of silicate glass passivation by surface layers. *Nature communications* 2015, *6*, (1), 6360.
34. Fournier, M.; Gin, S.; Frugier, P., Resumption of nuclear glass alteration: state of the art. *Journal of Nuclear Materials* 2014, *448*, (1–3), 348–363.
35. Vienna, J. D.; Ryan, J. V.; Gin, S.; Inagaki, Y., Current understanding and remaining challenges in modeling long-term degradation of borosilicate nuclear waste glasses. *International Journal of Applied Glass Science* 2013, *4*, (4), 283–294.
36. Gin, S.; Frugier, P.; Jollivet, P.; Bruguier, F.; Curti, E., New insight into the residual rate of borosilicate glasses: effect of S/V and glass composition. *International Journal of Applied Glass Science* 2013, *4*, (4), 371–382.

37. Gin, S.; Beaudoux, X.; Angéli, F.; Jégou, C.; Godon, N., Effect of composition on the short-term and long-term dissolution rates of ten borosilicate glasses of increasing complexity from 3 to 30 oxides. *Journal of Non-Crystalline Solids* 2012, *358*, (18–19), 2559–2570.
38. Hubert, M.; Faber, A. J., On the structural role of boron in borosilicate glasses. *Physics and Chemistry of Glasses-European Journal of Glass Science and Technology Part B* 2014, *55*, (3), 136–158.
39. Tournié, A.; Ricciardi, P.; Colomban, P., Glass corrosion mechanisms: A multiscale analysis. *Solid State Ionics* 2008, *179*, (38), 2142–2154.
40. Ledieu, A.; Devreux, F.; Barboux, P.; Sicard, L.; Spalla, O., Leaching of borosilicate glasses. I. Experiments. *Journal of Non-Crystalline Solids* 2004, *343*, (1–3), 3–12.
41. Peuget, S.; Maugeri, E. A.; Charpentier, T.; Mendoza, C.; Moskura, M.; Fares, T.; Bouty, O.; Jégou, C., Comparison of radiation and quenching rate effects on the structure of a sodium borosilicate glass. *Journal of Non-Crystalline Solids* 2013, *378*, 201–212.
42. De Bonfils, J.; Peuget, S.; Panczer, G.; De Ligny, D.; Henry, S.; Noël, P.-Y.; Chenet, A.; Champagnon, B., Effect of chemical composition on borosilicate glass behavior under irradiation. *Journal of Non-Crystalline Solids* 2010, *356*, (6–8), 388–393.
43. Lizzi, F.; Goutaudier, C.; Attik, N.; Jackson, P.; Campbell, I.; Mokbel, I.; Grosgogeat, B.; Villat, C., Ion release characterization in phase separated borosilicate glass powders. *Journal of Non-Crystalline Solids* 2020, *534*, 119934.
44. Angeli, F.; Villain, O.; Schuller, S.; Charpentier, T.; de Ligny, D.; Bressel, L.; Wondraczek, L., Effect of temperature and thermal history on borosilicate glass structure. *Physical Review B—Condensed Matter and Materials Physics* 2012, *85*, (5), 054110.
45. Bisbrouck, N.; Micoulaut, M.; Delaye, J.; Gin, S.; Angeli, F., Structure–property relationship and chemical durability of magnesium-containing borosilicate glasses with insight from topological constraints. *npj Materials Degradation* 2022, *6*, (1), 58.
46. Damodaran, K.; Gin, S.; Narayanasamy, S.; Delaye, J.-M., On the effect of Al on alumino-borosilicate glass chemical durability. *npj Materials Degradation* 2023, *7*, (1), 46.
47. Gin, S.; Mir, A. H.; Jan, A.; Delaye, J.-M.; Chauvet, E.; De Puydt, Y.; Gourgiotis, A.; Kerisit, S., A general mechanism for gel layer formation on borosilicate glass under aqueous corrosion. *The Journal of Physical Chemistry C* 2020, *124*, (9), 5132–5144.
48. Regnier, E.; Perret, D.; Vallat, C.; Mure, S.; Brackx, E.; Issoire, A.; Laplace, A., Incorporation of silver in borosilicate nuclear glass. *Materials Letters* 2025, *383*, 138026.
49. Narayanasamy, S.; Jollivet, P.; Jégou, C.; Moskura, M.; Abdelouas, A.; Charpentier, T.; Angeli, F., Borosilicate glass alteration in vapor phase and aqueous medium. *npj Materials Degradation* 2022, *6*, (1), 86.
50. Narayanasamy, S.; Bell, J. G.; Tiwari, S.; Charpentier, T.; Delaye, J.-M.; Cournède, É.; Thill, A.; Tache, O.; Lai-Kee-Him, J.; Ancelin, A., Insights into gel maturation from alteration of borosilicate glass from 7 days to 27 years. *npj Materials Degradation* 2025, *9*, (1), 118.

51. Kerisit, S.; Pierce, E. M., Monte Carlo simulations of the dissolution of borosilicate and aluminoborosilicate glasses in dilute aqueous solutions. *Geochimica et Cosmochimica Acta* 2011, *75*, (18), 5296–5309.
52. Ledieu, A.; Devreux, F.; Barboux, P., Monte Carlo simulations of borosilicate glass corrosion: predictions for morphology and kinetics. *Journal of non-crystalline solids* 2004, *345*, 715–719.
53. Devreux, F.; Ledieu, A.; Barboux, P.; Minet, Y., Leaching of borosilicate glasses. II. Model and Monte-Carlo simulations. *Journal of Non-Crystalline Solids* 2004, *343*, (1–3), 13–25.
54. Kerisit, S.; Pierce, E. M.; Ryan, J. V., Monte Carlo simulations of coupled diffusion and surface reactions during the aqueous corrosion of borosilicate glasses. *Journal of Non-Crystalline Solids* 2015, *408*, 142–149.
55. Jabraoui, H.; Charpentier, T.; Gin, S.; Delaye, J.-M.; Pollet, R., Behaviors of sodium and calcium ions at the borosilicate glass–water interface: Gaining new insights through an ab initio molecular dynamics study. *The Journal of Chemical Physics* 2022, *156*, (13).
56. Jabraoui, H.; Charpentier, T.; Gin, S.; Delaye, J.-M.; Pollet, R., Atomic insights into the events governing the borosilicate glass–water interface. *The Journal of Physical Chemistry C* 2021, *125*, (14), 7919–7931.
57. Gin, S.; Guo, X.; Delaye, J.-M.; Angeli, F.; Damodaran, K.; Testud, V.; Du, J.; Kerisit, S.; Kim, S. H., Insights into the mechanisms controlling the residual corrosion rate of borosilicate glasses. *Npj Materials Degradation* 2020, *4*, (1), 41.
58. Tan Shengheng.; Chang Jing.; Wang Jiateng.; He Cheng.; Li Yang.; Wang Changfu.; Zhang Hua.; Long Haoqi., Study on the reaction process between calcined products of spent liquid from dynamic stacking and glass matrix during melting. *Atomic Energy Science and Technology*, 2025, 59(1): P.46–56, 11.
59. Lichtner, P. C.; Hammond, G. E.; Lu, C.; Karra, S.; Bisht, G.; Andre, B.; Mills,R.; Kumar, J., *PFLOTRAN user manual: A massively parallel reactive flow and transport model for describing surface and subsurface processes*; Los Alamos National Laboratory (LANL), Los Alamos, NM (United States …
60. Chen, P.; Van Loon, L.R.; Koch, S.; Alt-Epping, P.; Reich, T; Churakov, S.V., Reactive transport modeling of diffusive mobility and retention of TcO4 – in Opalinus Clay. *Applied Clay Science* 2024, *251*, p.107327.

Figures

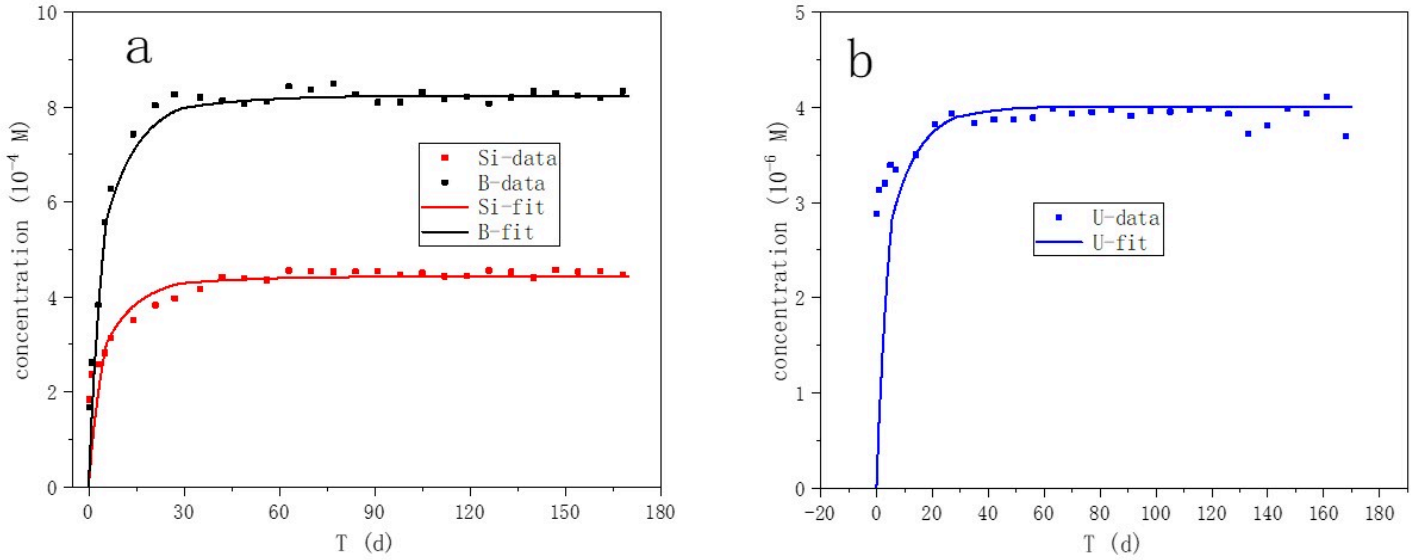


Figure 1

Best fit result of a) Si and B, b) U concentration in solution.

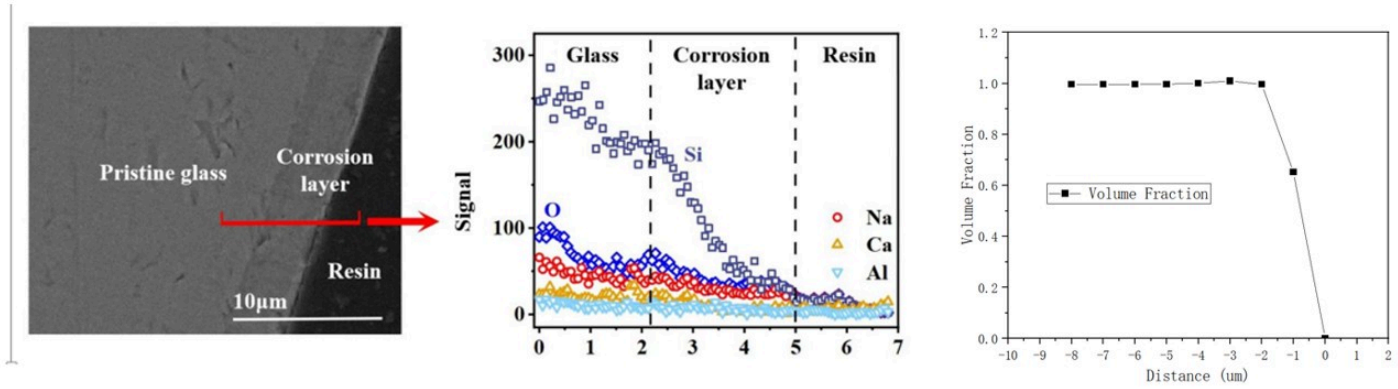


Figure 2

surface properties of borosilicate glass after leach experiment. a) morphology of leached glass surface by SEM; b) element distribution along line scan by SEM-EDX; c) volume fraction of glass after simulation by reactive leach model.

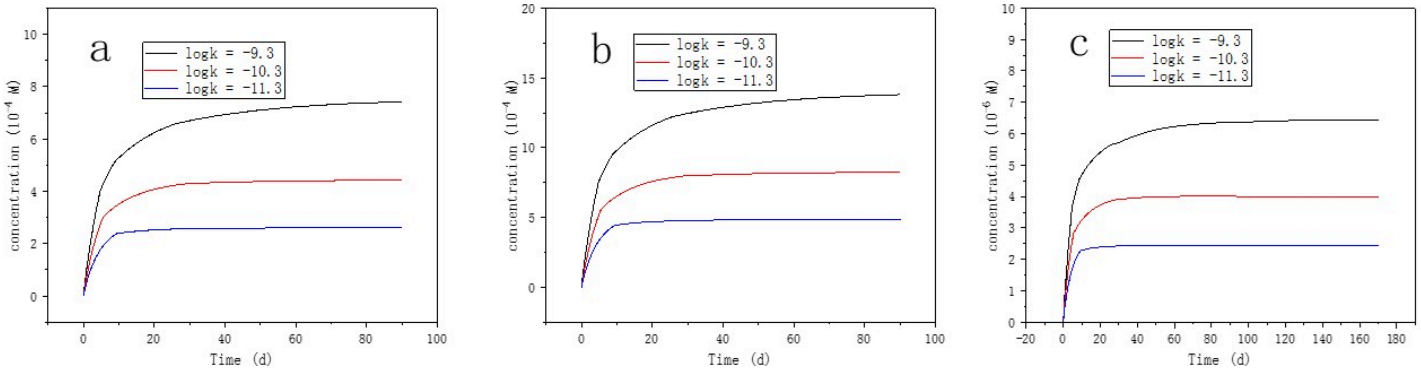


Figure 3

Impact of equilibrium constant, log K, on leached a) Si, b) B, and c) U in solution.

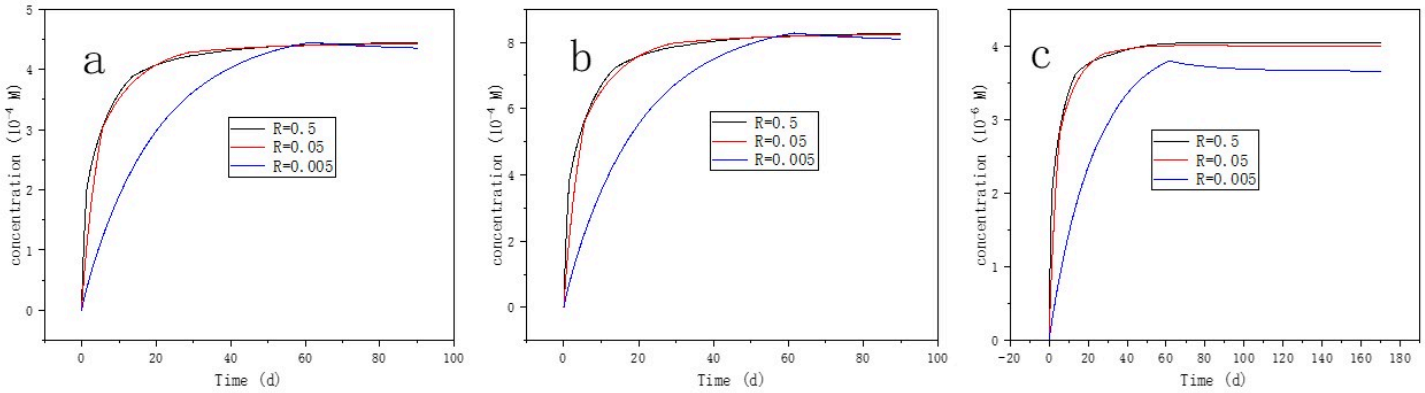


Figure 4

Impact of factors reaction rate, R, on leached a) Si, b) B and c) U in solution.

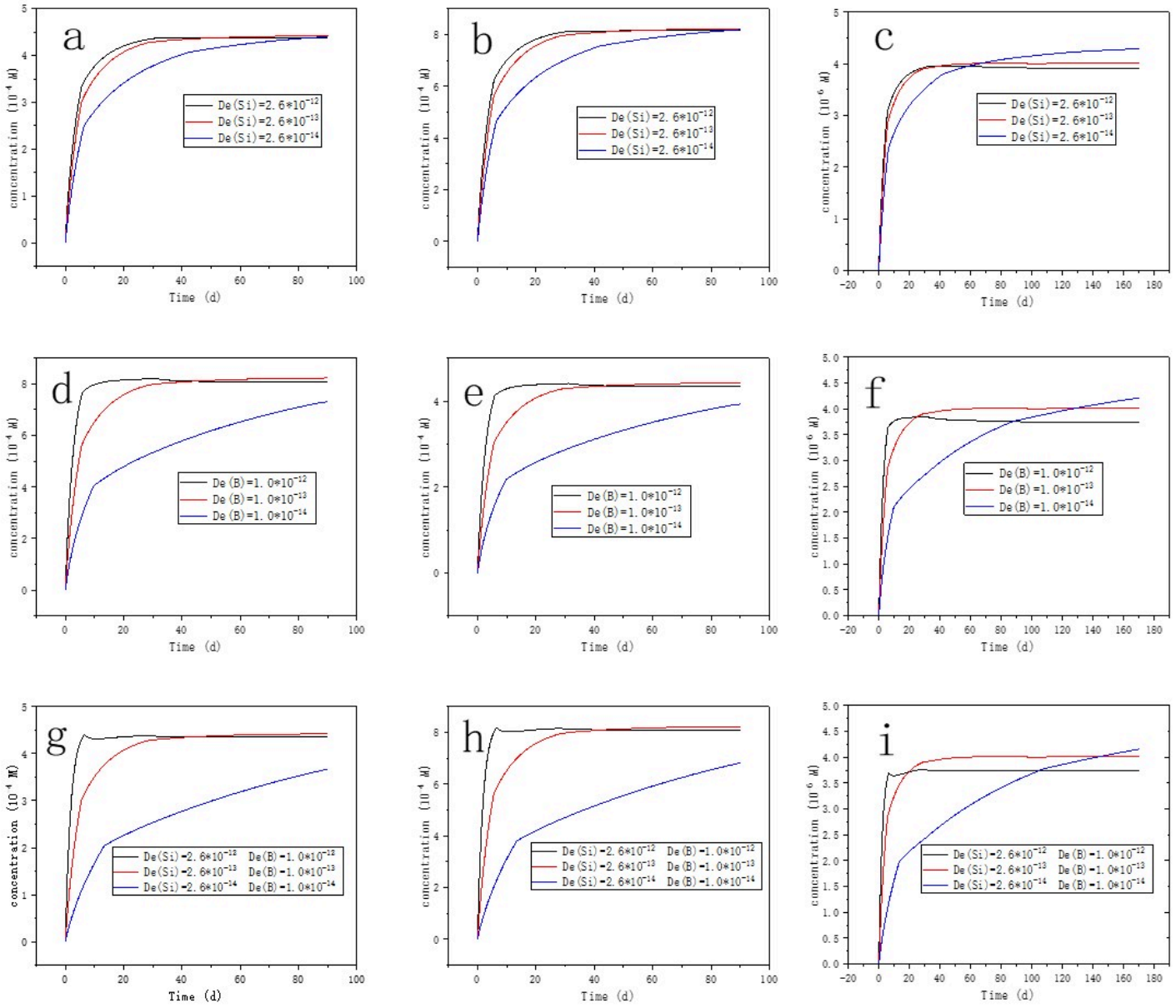


Figure 5

Impact of effective diffusion coefficient, D_e, on leached Si, B and U in solution. a) D_e of Si influence on Si; b) D_e of Si influence on B; c) D_e of Si influence on U; d) D_e of B influence on Si; e) D_e of B influence on B; f) D_e of B influence on U; g) D_e of both Si and B influence on Si; h) D_e of both Si and B influence on B; i) D_e of both Si and B influence on U.

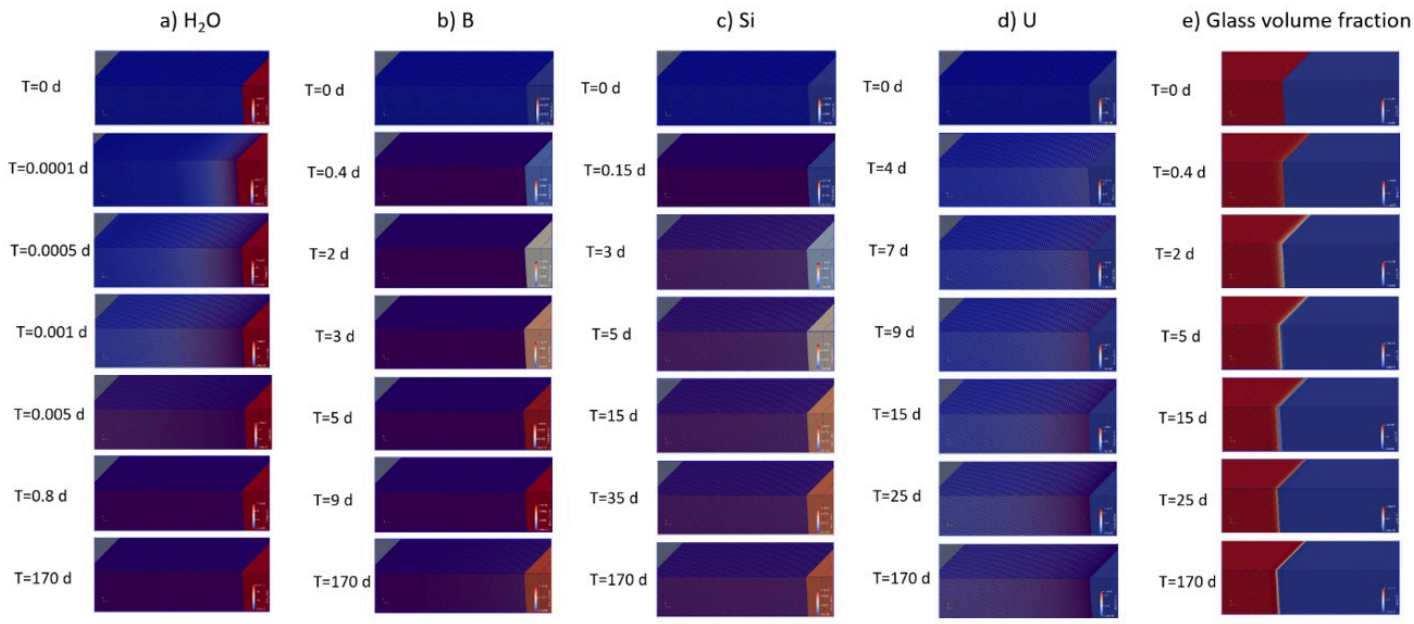


Figure 6

Concentration of a) H_2O, b) B, c) Si, and d) U e) glass volume fraction as function of time during leach process.

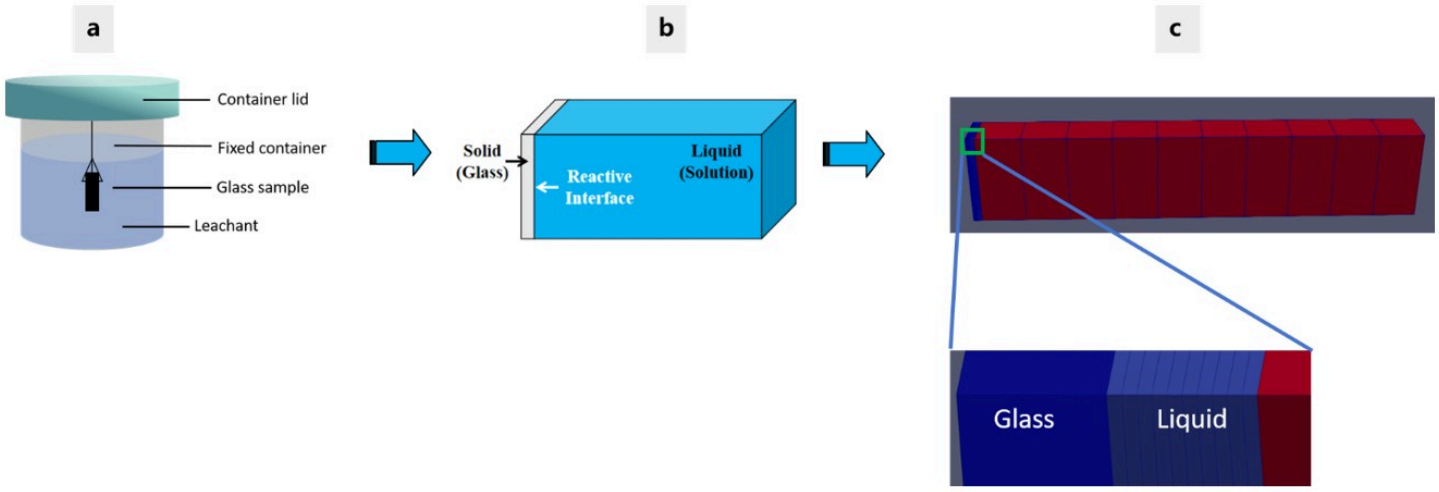


Figure 7

Geometry of leach model. a) Schematic view of leach experiment as described in above text. b) Cubic sliced glass leached from 6 faces was abstracted equivalent to 1 interface geometry. c) Grid of the geometry.

Supplementary Files

This is a list of supplementary files associated with this preprint. Click to download.

- supplementaryinformation.docx